Available online at www.sciencedirect.com

ScienceDirect

Procedia Manufacturing 40 (2019) 14–21

Procedia MANUFACTURING

www.elsevier.com/locate/procedia

19th Machining Innovations Conference for Aerospace Industry 2019 (MIC 2019), November 27th - 28th 2019, Hannover, Germany

Increasing productivity in heavy machining using a simulation based optimization method for porcupine milling cutters with a modified geometry

B. Denkena[a], A. Krödel[a], O. Pape[a]*

[a]*Institute of Production Engineering and Machine Tools, Leibniz Universität Hannover, An der Universität 2, D-30823 Garbsen, Germany*

* Corresponding author. Tel.: +49-511-76218259; fax: +49-511-7625115 *E-mail address:* pape@ifw.uni-hannover.de

Abstract

Porcupine milling cutters offer a high potential for increasing the metal removal rate in heavy machining of steel and titanium. Here, the available machine power and the maximum radial force represent important process limits. According to the current state of the art, mainly rectangular indexable inserts are used. Investigations show that the use of round inserts can significantly reduce the resulting radial force and cutting torque similar to serrated endmills. However, the design of such tools is a major challenge due to the complicated shape of cross-section of the undeformed chip. Therefore, this paper presents a new method for optimizing the position of individual indexable inserts by means of geometric material removal simulations. With the new method, the radial force can be reduced by 14%.

Keywords: tool optimization, milling, simulation

1. Introduction

Porcupine milling cutters are used in high-performance cutting (HPC) to maximize the metal removal rate during the roughing process of large components (Fig. 1 a). Typical applications are the machining of integral titanium components in the aerospace industry [1, 2] and components made of high-alloy steels for the energy sector such as components for diesel power plants or cast housings for wind turbines.

When machining with porcupine milling cutters with diameters up to 80 mm, high mechanical loads like process forces of up to 50 kN and cutting torques of 1000 Nm occur [3]. Today, the tool load represents a process limit for increasing productivity, due to the limited stiffness and tensile strength of the tool body and machine tool.

According to the current state of the art, only rectangular indexable inserts are used, which lead to a flat surface. However, preliminary studies show that the radial force and the cutting torque is significantly reduced by using round indexable inserts (Fig. 1 b) [4].

10.1016/j.promfg.2020.02.004

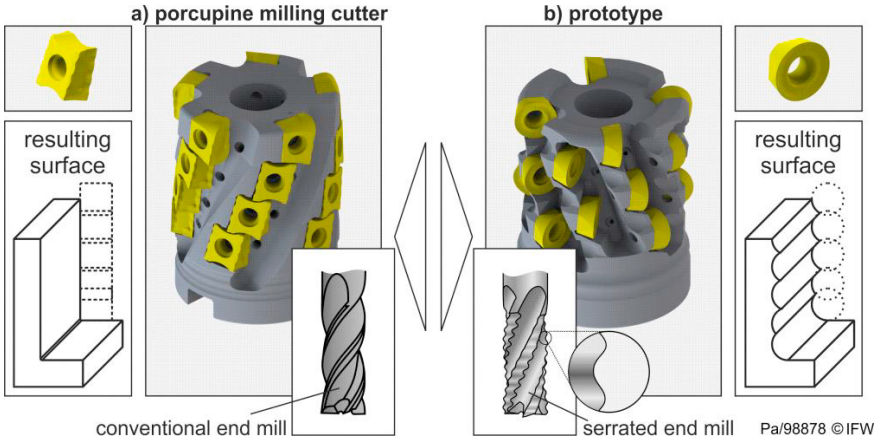

Figure 1: Porcupine milling cutters

Thus, this approach adapts the positive effects of serrated end mills to porcupine milling cutters. Here, the main mechanism of the cutting force reduction is the decreased contact length between the tool and workpiece [5]. The same affect can also be applied when using round instead of rectangular inserts. The resulting surface, which is no longer flat, is acceptable, because the following finishing operations will remove the excess material in subsequent steps. With the investigated prototype, the maximum peak height of the excess material is 1 mm. Thus, it is expected that tool wear and machining time of subsequent tools will not be affected.

Nevertheless, little is known about the optimal tool geometry. In addition, the engagement between tool and workpiece is more complicated than with conventional tools, making the design and optimization of such tools a challenging task. This paper presents a new way to determine the positions of individual indexable inserts in order to minimize the cutting torque and radial force. Therefore, this paper is divided into four parts. First, experimental tests are carried out to calibrate a suitable force model for both, the conventional and the prototype tool. Second, a new method to optimize the positions of individual indexable inserts is presented. Third, the results of the optimization are discussed. As a last step, the optimized toot geometry is manufactured and cutting tests are carried out to validate the optimization and show the potential of the prototype.

2. Experimental setup

All experimental tests were performed on a Heller H5000 machine tool with a maximum torque of M_{max} = 2292 Nm and a maximum spindle power of P_{max} = 60 kW. Figure 2 shows the experimental setup for the cutting experiments. Here, the workpiece made of Ti-6Al-4V (beta-annealed) is directly mounted on a dynamometer type 9255C from Kistler (Fig. 2 a). Beside the force measurements in three directions, the effective spindle power is also recorded directly in the machine control (Fig. 2 b).

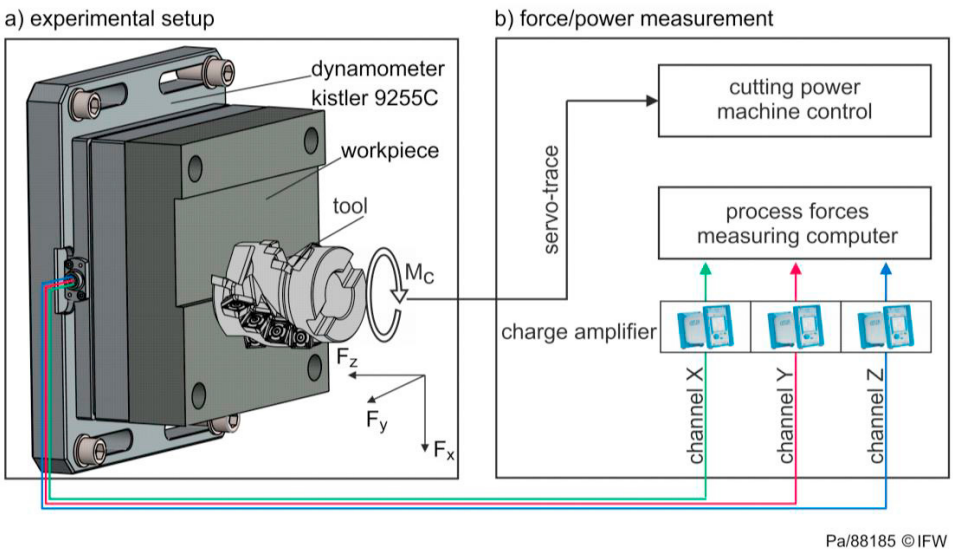

Figure 2: Experimental setup

The experimental investigations consist of two parts. As a reference, cutting tests with the tool type M3255-050-B22-05-46 and indexable inserts of the type P4500-7461332 from Walter AG are carried out. Afterwards, force measurements with round inserts are conducted with a stepwise increasing feed to calibrate the force model from Altintas et al. [6, 7] according to the method presented by Gradisek et al. [8]. However, no conventional porcupine milling cutters with round inserts exist. Therefore, conventional shoulder milling cutters type F2334R.B22.050.Z05.06 with inserts of the type ROMX1204M0-F67 WSM45X are used. The process parameters for both tools are shown in table 1.

Table 1. Process parameters for the cutting tests

Process parameter	Reference tool	Shoulder milling cutter with round inserts
Axial depth of cut a_p	40 mm	8 mm
Radial depth of cut a_e	30 mm	30 mm
Feed per tooth f_z	0.12 mm	0.04, 0.08, 0.12, 0.16, 0.20 mm
Cutting speed v_c	45 m/min	45 m/min

The results of the cutting tests using a stepwise increasing feed and shoulder milling cutter with round inserts are shown in (Fig. 3 a)). For each feed, the force was measured in three spatial directions and the mean values were calculated. The regression lines for the force model from Altintas et al. are shown in (Fig. 3 b). With a maximum error of 5%, they are in good agreement with the measured values. The result is a calibrated force model for the optimization of the tool geometry of porcupine milling cutters with round indexable inserts.

3. Design of the novel tool geometry

When designing a new tool, the parameters of the tools geometry must be defined first. The geometry parameters are the degrees of freedom for the following optimization. To be able to manufacture the tool body, the parameters cannot be selected randomly. Therefore, constraints for the tool geometry have to be formulated. Then, the forces can be calculated individually for each unique tool geometry using the calibrated force model from the last chapter and a suitable material removal simulation.

3.1. Selection of parameters

The indexable inserts of porcupine milling cutters are arranged in rows forming the cutting edges (Fig. 4). Within a row, consecutive inserts are further arranged with an axial offset Δz and an angular offset ΔΦ.

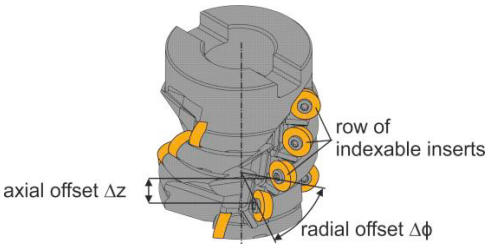

Figure 3: Tool geometry of porcupine milling cutters

The orientation of the indexable insert with a tool cutting edge inclination of $\lambda_s = 5°$ and a tool cutting edge angle of $\kappa_r = 2.8°$ was adopted from the shoulder milling cutter and remain unchanged. Therefore, the coefficients for the force model obtained in the experiments with the reference tool are assumed to be constant. This ensures that the force coefficients of the shoulder milling cutter can also be applied to the prototype. Furthermore, the substrate and micro-geometry with a symmetrical cutting edge rounding of $r_\beta = 30$ µm of the round inserts is the same as that of the tangential inserts. As a result, the specific friction forces and tool wear are approximately the same for both, the reference and prototype porcupine milling cutter.

The round inserts lead to a sickle-shaped cross section of undeformed chip (Fig. 5 a). This cross section shape has three disadvantages: First, a larger part of the cutting edge is engaged compared to conventional squared inserts, thus the friction force of such tools increases.

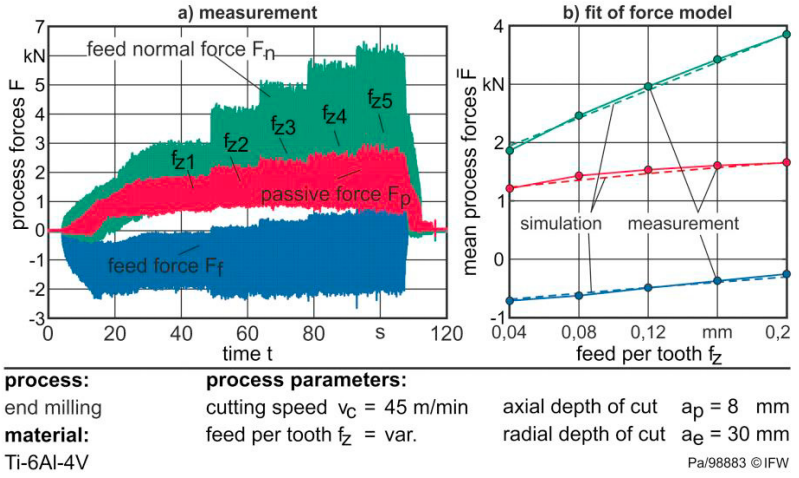

Figure 4: Experimental results

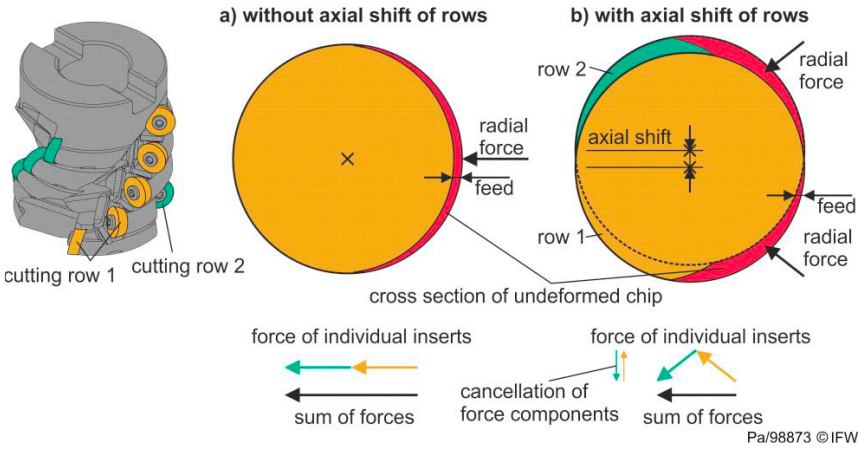

Figure 5: Cross section of undeformed chip

Second, the chips are stiffer due to the higher surface moment of inertia, which results in a disadvantageous chip formation due to a less curled chip. Third, the radial force mainly acts perpendicular to the tools axis, thus increasing the bending moment of the tool body. Therefore, a small axial shift of consecutive rows is necessary and has to be considered as an additional parameter (Fig. 5 b). This shift distributes the chip cross section more to the side of the round inserts. As a result, the chip thickness is increased and the engaged cutting edge length is decreased. This leads to a reduction of the friction force. Furthermore, the radial force acts more towards the axial direction, where the axial force components of two subsequent inserts are cancelled out (Fig. 5). In summary, the axial and radial offset and the shift of successive rows are selected as influencing variables in tool optimization.

3.2. Calculation of boundary conditions

In order to be able to manufacture the tool body and to ensure enough space for the chips, certain limitations regarding the parameters of the tool geometry exist. However, according to the current state of the art, there is no method for determining the limits of the possible tool geometry. Therefore, a new approach is presented in this paper. As a first step, a two-dimensional boundary curve around an indexable insert is defined (Fig. 6 a). Due to the simple mathematical description, ellipses with the main axes a and b were chosen. These curves are then projected onto the cylindrical envelope of the tool body according to the individual positions of the inserts (Fig. 6 b). It should be noted that the position of the insert within the ellipse does not need to be determined, because only the relative position between different ellipses is relevant. After the projection, all ellipses are checked for intersections in cylindrical coordinates. If there is more than one intersection point between two ellipses, the tool geometry is invalid. This method is applicable for all tool geometries. Furthermore, the calculation is independent of the tool diameter due to the projection.

In the present case, an ellipse with parameters a = 19.6 mm and b = 12.2 mm was selected for the round inserts. The parameter a provides an angular distance of 45° with a tool diameter of 50 mm. The parameter b was defined by the diameter of 12 mm of the insert including a tolerance of 0.2 mm.

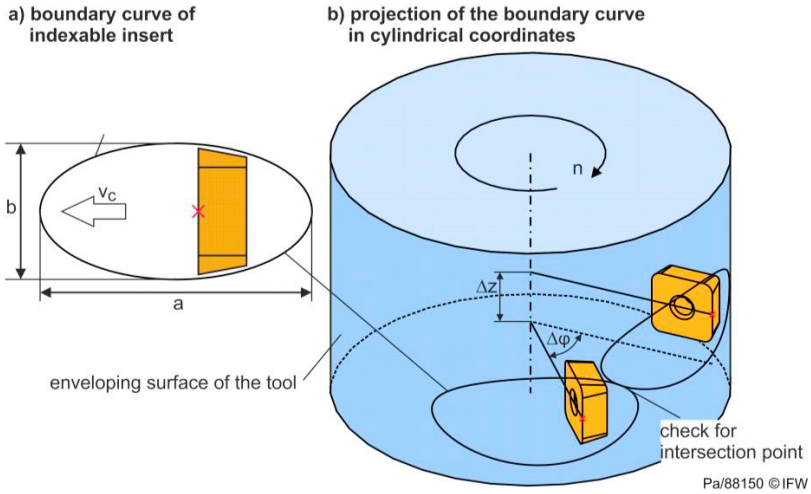

Figure 6: Calculation of the limiting tool geometries

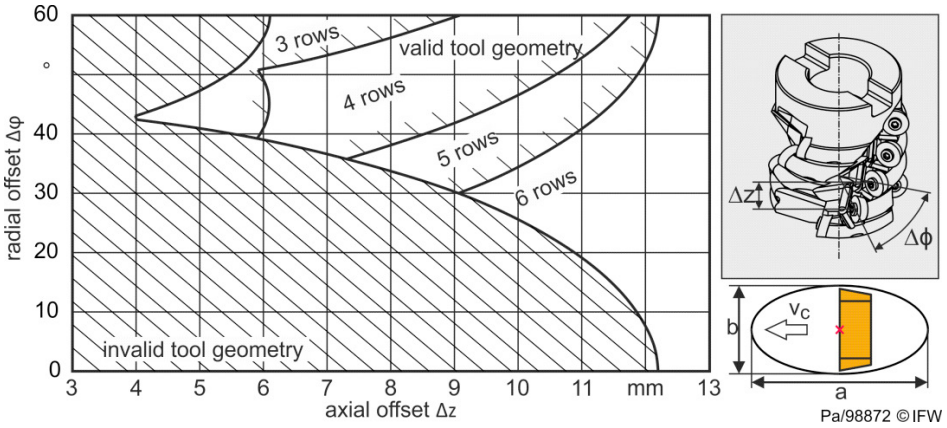

Figure 7: Range of possible tool geometries

Figure 7 shows the range of possible tool geometries for different axial and radial offsets and different numbers of rows of teeth. The limit curves show a complicated piecewise defined nonlinear course although a mathematically simple ellipse formulation was used. With an increasing number of rows, the area of possible tool geometries is decreasing. In summary, this approach can be used to check the manufacturability of a large parameter range of different geometries.

3.3. Simulation approach

In contrast to porcupine milling cutters with rectangular inserts, there is no analytical equation for the chip cross section of tool geometries with round inserts. Therefore, a numerical solution is needed for the cross section and the following force calculation. In the present case, a multi-dexel-based material removal simulation is used [9]. Here, the dexels are intersected with the tools surface, which consists of small quadrilaterals near the cutting edge (Fig. 8). The cross section is further derived from the enveloping curve of all intersection points [9]. A similar approach for a cutting edge discrete intersection calculation can be found in [10]. With this approach, arbitrary tool geometries can be investigated for the following optimization. It should be mentioned that in Fig. 8, only one dexel direction is drawn for better representation, whereby three redundant dexel fields aligned to the coordinate axes were used in the simulation.

4. Optimization

During the following optimization, the maximum magnitude of the radial force is selected as a target parameter. For the reference tool, a maximum radial force of 14.7 kN was measured, which leads to high stresses in the tool body. This has been identified as a limiting factor in the experimental investigations, because the measured cutting power P = 9 kW and the cutting torque M = 300 Nm do not reach the limits of the machine (M_{max} = 2292 Nm, P_{max} = 60 kW). The force coefficients obtained from the cutting test with round indexable inserts where used for the force calculation. The radial offset Δφ, axial offset Δz and the axial shift Δs between individual rows are selected as the degrees of freedom, which were varied according to Table 2. The number of rows is kept constant at four. This leads to a rotationally symmetrical arrangement of the inserts with an axial shift greater than zero. It should be

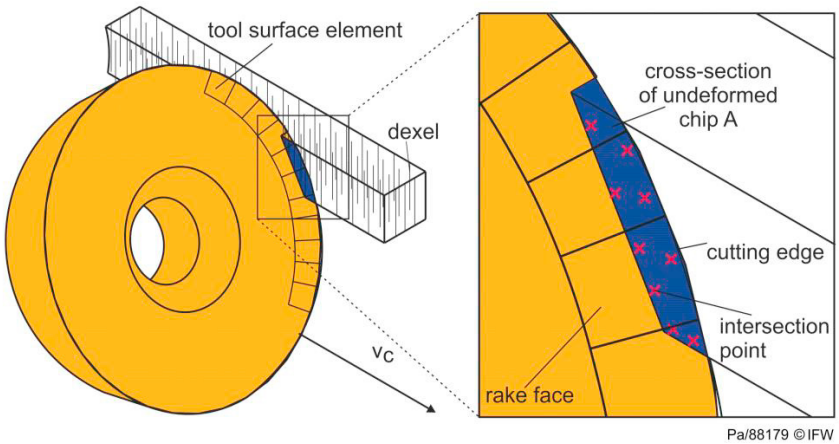

Figure 8: Material removal simulation

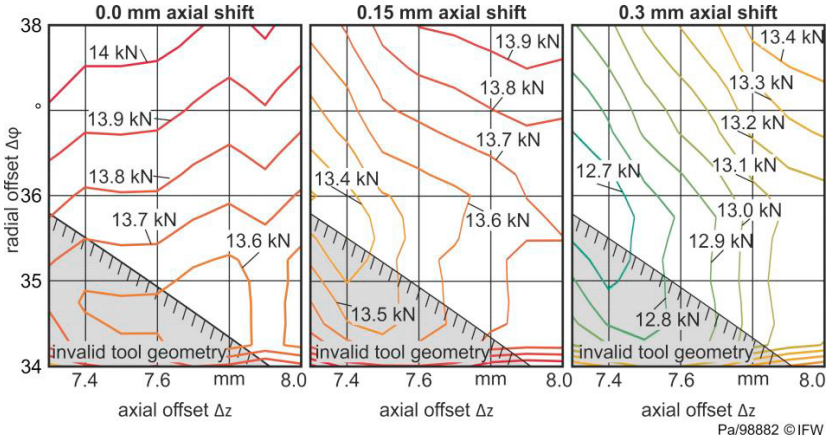

Figure 9: Results of the force calculation

mentioned that the reference porcupine milling cutter has five rows. Therefore the simulations are carried out with a feed per tooth of $f_z = 0.15$ mm instead of $f_z = 0.12$ mm of the reference to get the same productivity.

Table 2. Variation of tool parameters

tool parameter	starting value	endvalue	increment
Angle offset Δφ	34°	38°	0.25°
Axial offset Δz	7.3 mm	8.0 mm	0.1 mm
Axial shift Δs	0 mm	0.3 mm	0.05 mm

The parameter range results in 952 individual simulations, which took about three days to calculate on an Intel Core i7 4790 processor. Unfortunately, the maximum value of the radial force is sensitive to discretization errors. Therefore, a high dexel resolution of 0.025 mm and an angular step of the tool of 0.5° are necessary for convergence. The results of the force calculation are presented in Fig. 9.

The maximum radial force is shown as a function of the radial and axial offset for three different axial shifts. In addition, the limit for a valid tool geometry is marked, which is independent of the axial shift in the present case, because consecutive rows of inserts do not intersect in the investigated parameter ranges. According to the simulated results, the measured radial force $F_{r,max} = 14.7$ kN of the reference tool can be decreased even when the axial shift is equal to zero. As described in the previous chapter, the radial force is additionally reduced by the axial shift, where the optimum is shifted to lower axial and to higher radial offsets. As a result, an optimum was found in the valid domain at $\Delta\varphi = 35.8°$, $\Delta z = 7.4$ mm and $\Delta s = 0.3$ mm. Unfortunately, the maximum chip thickness increases with an axial shift of 0.3 mm up to a value of $h_{max} = 0.28$ mm compared to $h_{max} = 0.15$ mm without an axial shift. Nevertheless, the maximum force, which acts on a single indexable insert is lower compared to the reference tool, because the total force is decreased and the number of inserts is kept constant. With the optimized tool parameters (Table 3), a tool body was designed (Fig. 10).

Figure 10: Designed tool body

Table 3. Final tool parameters of the prototype

tool parameter	value
Angle offset Δφ	35.8°
Axial offset Δz	7.4 mm
Axial shift Δs	0.3 mm
Number of rows	4
Inserts per row	5
cutting edge inclination of λ_s	5°
tool cutting edge angle of κ_r	2.8°

5. Experimental test with the new tool geometry

The designed tool body was manufactured and cutting test were carried out with the exact same process parameters of the reference tool and the simulations during the optimization (Fig. 11). As a first result, the tool body was sufficiently dimensioned to withstand the loads. Also, the chip spaces were large enough for sufficient chip removal. Thus, the calculation method for a valid tool geometry leads to useful results. However, due to the sharp workpiece geometry at the edge, burr formation can be observed (Fig. 11). In order to remove this, further inserts will be added in the next iteration.

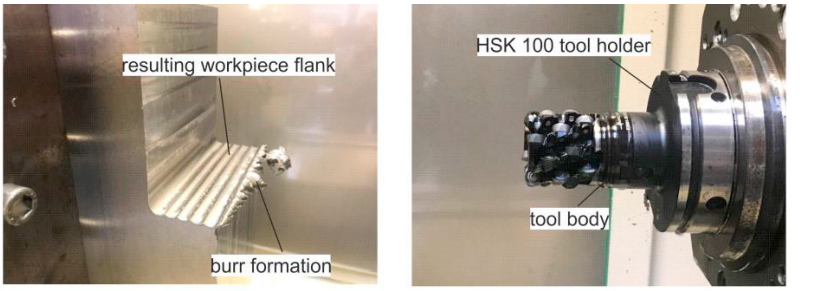

Figure 11: Experimental cutting tests

As a second step, the radial force was measured and compared to the simulations with the force coefficients obtained from the shoulder milling cutter (Fig. 12). Here, the simulation results are in good agreement with the measurement for the first half of the tool rotation. However, during the second half of the tool rotation, slight deviations are visible. These probably result from the manufacturing tolerances of the indexable inserts and insert seats as well as from a runout of the tool body in the holder.

As a final result, a maximum radial force of 12.71 kN was measured along the complete tool path. This is only slightly above the simulated optimum of the maximum radial force of 12.68 kN, which validates the optimization. Compared to the observed maximum of the reference porcupine milling cutter with $F_{r,max}$ = 14.7 kN, the novel tool geometry reduces the force by 14%. Theoretically, the cutting depth can be increased to 45 mm until the prototype has the same maximum radial force.

6. Conclusion and outlook

In this study, a new approach is presented, which supports the design and optimization process of complex cutting tools. This method has been used to analyze a novel tool geometry developed at the Institute of Production Engineering and Machine Tools (IFW), which transfers the shape of serrated endmills to porcupine milling cutters. The high nonlinearity of the relation between the process force, boundary conditions and tool geometry shows the necessity of the approach. Finally, the simulation results were validated in experimental investigations, whereby the maximum radial force as a process-limiting factor could be reduced by 14%.

In future work, the identified optimal tool geometry will be further optimized in a second optimization loop. Here, the radial and axial offsets as well as the axial shift are not regarded as constant but are set individually for each indexable insert as a degree of freedom. In addition, the peak height of the resulting surface as well as the burr formation are included as additional optimization variables.

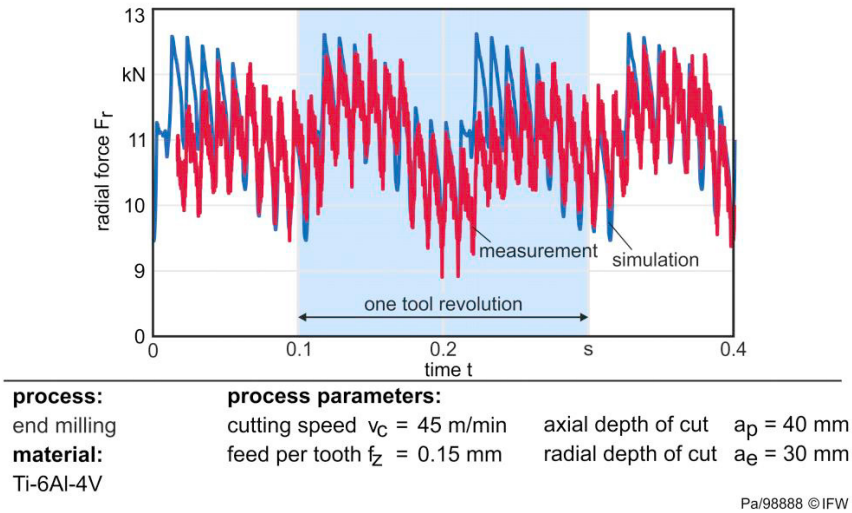

Figure 12: Simulated and measured radial force

Acknowledgements

The IGF-project (IGF – 19654 N WSF) of the Research Association (FGW) was supported by the AiF within the program for the promotion of industrial research (IGF) from the Federal Ministry of Economy and Energy due to a decision of the German Bundestag. The authors would like to thank the project partners for their support and the Walter AG for providing the cutting tools and producing the prototypes.

References

[1] Lange, M.: HPC of Aluminum and Titanium Aircraft Components – Challenges and Trends, 6. Machining Innovations Conference, Hannover, 2015, pp. 4-15

[2] Lütjering G., Williams, J.C.: Titanium, Springer, Berlin, 2007

[3] Heuwinkel, M.: Innovative Machining Strategies for Aerospace Components, 5. Machining Innovations Conference, Hannover 2014, pp. 150-169

[4] Denkena B, Nespor D.: Fräswerkzeug , Patent specification, German Patent and Trademark Office 2017, DE 102016104005 A1, Publication date: 07.09.2017.

[5] Tehranizadeh F, Budak E.: Design of Serrated End Mills for Improved Productivity. 16th CIRP Conference on Modelling of Machining Operations. 2017, pp. 493 - 498

[6] Engin S., Altintas Y.: Mechanics and dynamics of general milling cutters Part I: helical end mills. International Journal of Machine Tools and Manufacture 41, 2001, pp. 2195-2212 .

[7] Engin S., Altintas Y.: Mechanics and dynamics of general milling cutters. Part II: inserted cutters. International Journal of Machine Tools and Manufacture 41, 2001, pp. 2213–2231

[8] Gradisek J., Kalveram M., Weinert K.: Mechanistic identification of specific force coefficients for a general end mill. International Journal of Machine Tools and Manufacture 44, 2004, pp. 401-414

[9] Boess V, Ammermann C, Niederwestberg D, Denkena B. Contact Zone Analysis Based on Multidexel Workpiece Model and Detailed Tool Geometry Representation. 3rd CIRP Conference on Process Machine Interactions, 2012, pp. 41-45

[10] Erkorkmaz K, Katz A, Hosseinkhani Y, Plakhotnik D, Stautner M, Ismail. Chip geometry and cutting forces in gear shaping. CIRP Annals 65/1, 2016, pp. 133-136